Radiation Physics and Chemistry 81 (2012) 512–518

Contents lists available at SciVerse ScienceDirect

Radiation Physics and Chemistry

journal homepage: www.elsevier.com/locate/radphyschem

Novel sol–gel methodology to produce $LaCoO_3$ by acrylamide polymerization assisted by γ-irradiation

G. Carabalí [a,b,*], E. Chavira [c], I. Castro [c], E. Bucio [b], L. Huerta [c], J. Jiménez-Mier [b]

[a] Instituto de Ciencias Nucleares, Universidad Nacional Autónoma de México, Circuito Exterior s/n, 70-360, 04510 México D.F., México
[b] Instituto de Ciencias Nucleares, Universidad Nacional Autónoma de México, 70-543, 04510 México D.F., México
[c] Instituto de Investigaciones en Materiales, Universidad Nacional Autónoma de México, 70-360, 04510 México D.F., México

ARTICLE INFO

Article history:
Received 8 February 2011
Accepted 30 January 2012
Available online 3 February 2012

Keywords:
Sol–gel reaction
Polyacrylamide
Thermochemical initiator
Gamma radiation
Semiconductor material $LaCoO_3$

ABSTRACT

In this paper we report the synthesis of $LaCoO_3$ (LCO) nano-particles with two methodologies: the conventional sol–gel reaction of acrylamide (AA) polymerization using a cross-linking agent (methylenebisacrylamide or MBA) with the activation of the polymerization reaction by thermo-chemical initiator (azobisisobutyrnitrile or AIBN). The second was a novel sol–gel methodology in which the polymerization of AA monomers was done without MBA and the initiation was achieved by gamma radiation. With thermochemical initiator a xerogel with a foam and porous structure was obtained, while the gamma-irradiation of the mixture leads to the formation of a compact resin with entrapped cations. X-ray diffraction (XRD) shows that formation of the product begins around 500 °C and according to analysis of microscopy images of powders calcined in 700 °C the average sizes of particles are 20 nm and 42 nm for samples obtained using γ-irradiation and AIBN as initiators, respectively. TEM images also show differences in particle morphology. Those synthesized using AIBN as initiator are dispersed, while those with γ-irradiation are in aggregates.

1. Introduction

In recent years, the majority of research in synthesis of materials has concentrated on the preparation and characterization of single phase of nano-sized compounds using wet chemical methods. More recently the field of interest has focused in sol–gel methodologies to produce a broad kind of ceramic material, because of their interesting catalytic, electrical and optical properties.

Among the most studied ceramic materials are the mixed oxides with the Perovskite structure ABO_3, which have been extensively investigated because of their interesting physical properties (Peña and Fierro, 2001). This is the case of the lanthanum cobaltite $LaCoO_3$ (LCO), a semiconductor (Chainani et al., 1992; Haas et al., 2004) that has shown interesting catalytic properties (Voorhoeve et al., 1977; Kim et al., 2010; Colonna et al., 2002). The most common method used for the synthesis of ceramic materials is the solid state reaction (SSR). To produce materials with SSR, it is necessary to perform successive millings of the powder and also to heat the sample to elevated temperatures by long periods. This results in inhomogeneous materials, which in some cases have unwanted phases with larger grain size and low superficial area (Sin and Odier, 2000).

The limitation to produce powders with small grain size has been overcome by introduction of various wet-chemical reactions or sol–gel methodologies that have been developed to prepare high quality and homogenous products. These methods are based on the principle that the reactants are mixed at the molecular level. Low calcination temperature is then needed to produce fine powders with higher surface area and high purity (Sin and Odier, 2000; Brinker and Scherer, 1990).

An interesting sol–gel route used to prepare nano-particles of ceramic materials is the chemical reaction of polymerization of the acrylamide (SGPA) (Sin and Odier, 2000; Cheng et al., 2008; Sin et al., 2003; Herrera et al., 2008; Calleja et al., 2011), which is also interesting because it is cheap and can be performed at large scales (Calleja et al., 2002). The most important step in the SGPA method is the creation of a polymeric gel, which is an array of crosslinked acrylamide chains forming a network. The polymerization of acrylamide proceeds via a free-radical mechanism, which is activated by the thermo-initiator α,α-azoisobutyronitrile (AIBN) and to promote the formation of the gel, the cross-linking agent *N,N′*-methylenebisacrylamide (MBA) is added (Sin and Odier, 2000). Cheng et al., (2008) reported the synthesis of LCO nano-particles by a similar method and they found that the particle size of LCO is modulated by the variation between cation concentration and total amount of organic precursors (acrylamide and crosslinking agent) in the mixture.

* Corresponding author at: Instituto de Ciencias Nucleares, Universidad Nacional Autónoma de México, Circuito Exterior s/n, 70-360, 04510 México D.F., México. Tel.: +52 55 56 22 46 72; fax: +52 55 56 16 22 33.
E-mail address: giovanni.carabali@nucleares.unam.mx (G. Carabalí).

0969-806X/$ - see front matter © 2012 Elsevier Ltd. All rights reserved.
doi:10.1016/j.radphyschem.2012.01.039

Here, we report a new method for the preparation of LCO nanocrystals by a sol–gel methodology polymerizing the acrylamide monomer with γ-irradiation (γ-SGPA), which was done at room temperature and atmospheric pressure. In this method, the cationic metals and organic monomer are mixed homogeneously at the molecular level in solution. The γ-irradiation of the mixture leads to the formation of a polymeric resin with entrapped cations homogeneously dispersed. In the last stage of this new synthetic process, the decomposition of the organic matrix with heat treatment, leads to the formation of nanocrystals of the material. This new γ-SGPA method shows good results and more experiments should be performed to study the effect of dosage and concentration of monomers in the size and morphology of the final product. The results that are obtained with γ-SGAP are compared with the LCO particles synthesized using the SGAP method where the polymerization reaction begins by the effect of the chemical initiator AIBN.

2. Experimental procedure

2.1. Method of sol–gel acrylamide polymerization (SGAP)

The synthesis of fine $LaCoO_3$ powders was done using the acrylamide polymerization method reported by Sin and Odier (2000). The first stage is the dissolution of each cation in their stoichiometric ratio La_2O_3 (CERAC, 99.99%) and Co_2O_3 (Aldrich, 99.9%). These oxides were completely dissolved in 100 ml of distilled water in separated beakers. After their dissolution, the Co^{3+} and La^{3+} cations were complexed by the addition of ethylenediamine tetraacetic acid (EDTA) (Fluka, 99%), in the ratio 1:1 and the pH was adjusted in the range of 2–6 just to dissolve completely the elements into a clear solution. The solutions were mixed together at room temperature, then acrylamide monomer (AA) (Fluka, 99.9%) and the crosslinked agent *N,N*-methylenebisacrylamide (MBA) were then added to the mixture. The amounts of these two components in the reaction are usually expressed in terms their *T*/*C* ratio (Rüchel et al., 1978), in where T=((w/v)% of AA) and C=((w/v)% of MBA). To synthesize the materials in this work we used the ratio T/C=10/5. Finally, a few milligrams of a chemical initiator α,α′-azoisobutyronitrile (AIBN; Fluka 98%) was added to initiate the polymerization reaction. The AIBN initiates the polymerization in 80 °C and the final result was a red hydrogel.

To obtain a desiccate gel (xerogel), the acrylamide-hydrogel was placed inside a microwave oven (SEV-MIC IV) during 40 min operating at 600 W. In the interior of the oven there was a glass container into which a flow of argon (Ar) was supplied during the drying process. The Ar gas provides an inert atmosphere which avoids the ignition of the gel. This xerogel was grinded in an agate RM 100 mortar (model Retsch), and the powder was heated into a thermolyne 46100 furnace. In order to avoid a spontaneous autoignition of the xerogel during thermal treatment, carefully controlled the furnace temperature. The heating was done slowly with temperature increases in 100 °C steps up to 700 °C. In this stage important organic and amorphous materials are removed and nanocrystals are grown. Finally the powder was heated at 900 °C during 4 h to obtain 1.89 g (94.3%) of the sample.

2.2. Method of sol–gel acrylamide polymerization initiated with gamma irradiation (γ-SGAP)

To produce samples of $LaCoO_3$ by the γ-SGAP method, a similar procedure as described in Section 2.1 was followed. The same chemical reagents were used with the exception of the crosslinking agent MBA and the initiator of the polymerization reaction AIBN. The amount of acrylamide added to the cation mixture was ~10 g (10 w/v %). The resulting solution was placed in glass ampoules which were degassed by repeated freeze–thaw cycles and filled with argon to remove air. The ampoules were hermetically sealed by melting the thin top with an open flame. Finally, the ampoules were exposed to ^{60}Co γ-source (Gammabeam 651 PT, MDS Nordion) at room temperature, at a dose of 10.8 kGy. The final result was again a red hydrogel which was removed from the ampoules. The process of drying and the subsequent heat treatment was the same as the one described above.

3. Characterization techniques

In order to determine the temperature interval in which the reaction should be carried out, thermogravimetric analysis (TGA) was performed in a Hi-Res 2950 TGA (TA Instruments). Differential thermal measurements (DTA) were made in a 2910 DTA with a DTA 1600 cell (TA Instruments). About 5–6 mg the xerogel samples obtained by both SGAP and γ-SGAP methods were placed in alumina crucibles and heated starting at room temperature to 1000 °C. The temperature rate to carry out the analysis was set to 10 °C/min and the flow of air used was 100 ml/min. FTIR-ATR spectra of the calcined xerogel were analyzed using a Perkin-Elmer Spectrum 100 spectrometer (Perkin-Elmer Cetus Instruments, Norwalk, CT). XRD diffractograms were obtained on a Bruker-axs D8-advance diffractometer, with radiation of $\lambda_{(CuK)}$=1.5406 Å. Diffractograms were collected at room temperature in a range 15–90° with a step size of 0.02° and a time per step of 0.6 s. The morphology of the samples obtained was analyzed by SEM on a Cambridge-Leica Stereoscan 440 electron microscope. The micrographs were taken with a voltage of 20 kV, current intensity of 1000 pA and WD=25 mm. Samples for SEM analysis were prepared by depositing either the xerogel or the $LaCoO_3$ powder onto a SEM sample holder previously covered with carbon tape.

The analysis of X-ray photoelectron spectroscopy (XPS) was carried out in a VG Microtech ESCA2000 Multilab UHV system, with an Al Kα X-ray source ($h\nu$=1486.6 eV), operated at 11.7 kV, 16 mA beam and a CLAM4 MCD analyzer. The surface of the samples was etched for 10 min with 3.5 kV Ar^+ at 0.12 μA mm^{-2}. The XPS spectrum was obtained at 55° to the normal surface in the constant pass energy mode (CAE), E0=50 and 20 eV, for survey and high resolution scans, respectively. The atomic relative sensitivity factors (RSF) reported by Scofield (1976) were corrected by the transmission function of the analyzer and by the reference materials Co_3O_4 and La_2O_3. The peak positions were referenced to the background silver $3d_{5/2}$ photopeak at 367.30 eV (1.10 eV FWHM) and C 1s hydrocarbon groups at a central position of 285.00 eV.

4. Analysis of results

In sol–gel methodology it is important to carry out a thermal analysis of the starting materials to know its thermal behavior during the heating stage. TGA and DTA curves give useful information about of decomposition reaction of gel during calcinations processes. Fig. 1 shows the TGA and DTA curves of the powder xerogel precursor obtained by the γ-SGAP and SGAP methods.

Fig. 1a gives the trend of the TGA curves for both precursors. Some differences in the number of thermal events and in the percentage of weight losses can be noticed. For the xerogel obtained with the SGAP method, only 3 thermal events were

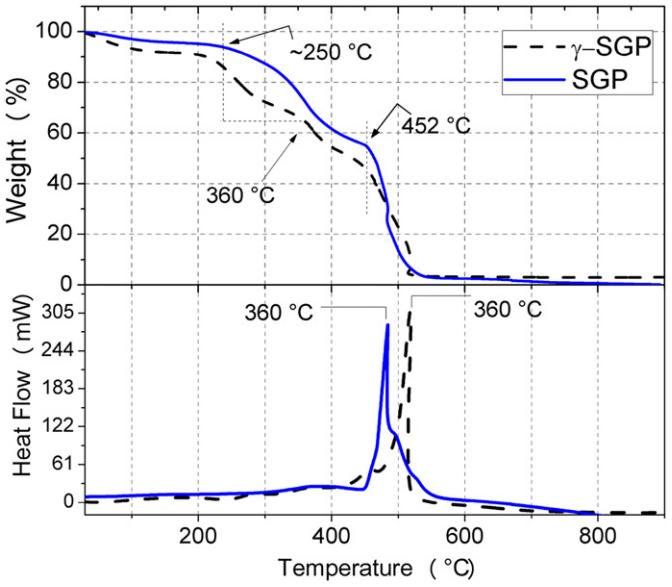

Fig. 1. TGA and DSC curves of xerogel powders synthesized by the γ-SGAP and SGAP methods.

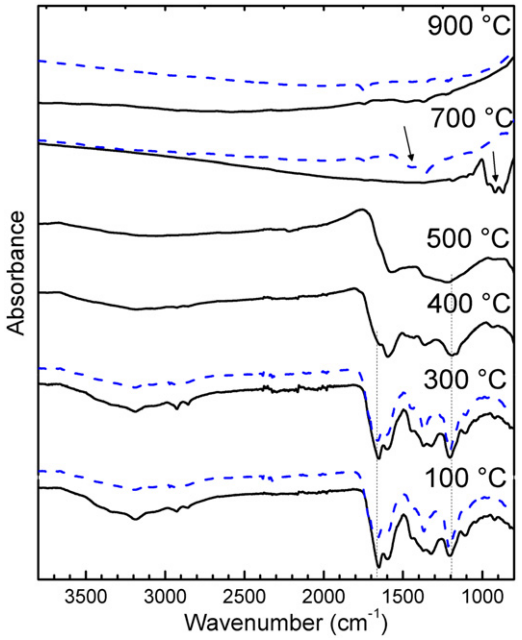

Fig. 2. FTIR spectra of the xerogels obtained by the γ-SGAP (solid line) and the SGAP (dashed line) methods and calcined at different temperatures (from 100 °C to 900 °C).

observed, whereas one additional between 250 and 360 °C appears for the γ-SGAP precursor. The first loss, occurring from the beginning until 250 °C, is due to dehydration and release of volatile substances. The second thermal event in the TG curve of γ-SGAP precursor is observed around 250 °C and 350 °C, but it is not clearly seen in the profile of the precursor obtained by the SGAP method. This event can be associated with the decomposition of EDTA in carbonates and nitrates (Herrera et al., 2009). The late thermal events, which have weight losses between 97% and 98%, are generated by the complete combustion of organic material of the polymer matrix. The calcination temperature of the organic material is different for the two precursors: in the precursor obtained by the SGAP method occurs at 482 °C, while for that obtained by the γ-SGAP method is about 518 °C (Fig. 1b).

Fig. 1b shows the DTA curves of SGAP and γ-SGAP precursors. A strong exothermic behavior in the range 300–550 °C was observed, which can be primarily associated with the burn out of organic species and the nitrate decomposition process. The temperature at which the total decomposition of organic matter was observed is different in both precursors. The maximum exothermic peaks in DTA curves of SGAP and γ-SGAP precursors are about 482 °C and 518 °C, respectively, and are due to thermal degradation of 97–98% of organic matter (according to TGA analysis). As it will be described in the following sections, in this temperature the amorphous component disappears and the crystallization process of the $LaCoO_3$ compound begins.

4.1. Fourier transforms infrared spectroscopy

In order to study the calcination processes of organic material, the xerogels obtained by the γ-SGAP and SGAP methods were slowly heated at different temperatures. FTIR spectra were used to observe the decomposition behavior of organic material. The FTIR spectra of the xerogel powders at different calcination temperatures are plotted in Fig. 2.

The FTIR spectra of the xerogel calcined at different temperatures show important changes: the wave numbers of the absorptions decrease gradually, bandwidths tend to increase and band numbers also decrease. These changes become visible when the heating temperature is increased. They are due to the decomposition process of organic material and the slow formation of the desired compound. The most intense bands in FTIR spectra are presented in three regions of spectrum: those at 2900–3500 are due to symmetrical and asymmetrical vibrations of the N–H groups, the ones at 1500–1700 are the main contribution for the characteristic bands belonging to the C=O vibration and those at 1100–1400 cm^{-1} are associated to the C–N vibration. Hydrogen bond formation between C=O and N–H groups produce considerable displacements of bands to the lower frequencies. Also it is important to consider that EDTA, some inorganic substances and high crosslinking effect in gel could produce significant differences in absorption bands of characteristic functional groups.

4.2. X ray diffraction

The crystallization behavior of solid precursors at different heat treatments was analyzed by X-ray diffraction. The γ-SGAP and SGAP xerogels were calcined in air at temperatures from 100 °C to 900 °C, maintaining each intermediate temperature for 12 h (Fig. 3). The XRD patterns of milled gel calcined at temperatures below 300 °C do not show any reflection peaks, which indicates that the powders are still amorphous. The formation of nanocrystals becomes evident at 500 °C. The crystal size of the powders synthesized by the γ-SGAP and SGAP methods and calcined at 600 and 900 °C were calculated using the Scherrer formula (Warren, 1990; Holzwarth and Gibson, 2011).

$$d = \frac{K\lambda}{\beta_{1/2}\cos\theta}$$

where K is the shape factor, λ is the X-ray wavelength (λ=1.5406 Å), β is the line broadening at half the maximum intensity (FWHM) in radians and θ is the Bragg angle. The value of dimensionless shape factor (K) considered in the calculations was 0.9 (it is important to note that the Scherrer formula is not always a reliable measure of particle size) (Warren, 1990; Holzwarth and Gibson, 2011). Table 1 shows the crystallite sizes calculated from XRD data using the Scherrer equation. All products obtained in this study were nanocrystalline with sizes of 16.1 and 25.3 nm for

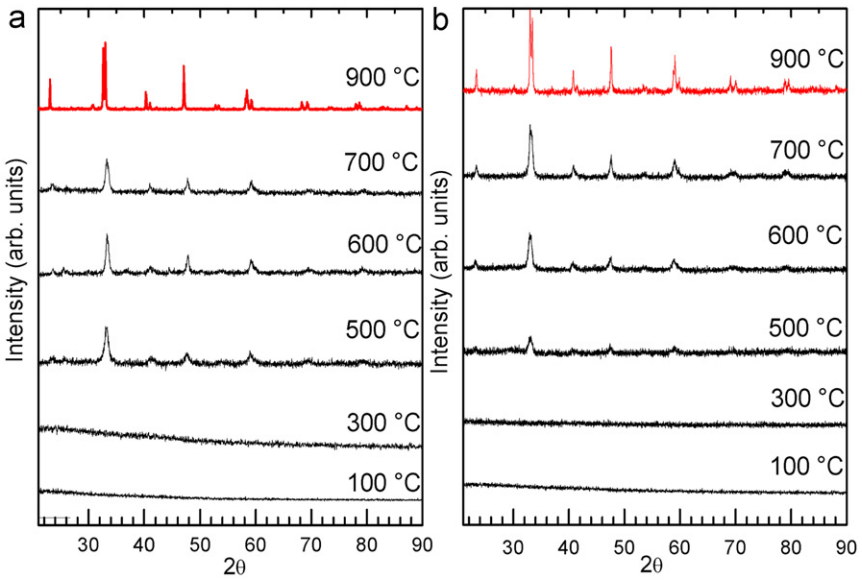

Fig. 3. XRD pattern of the xerogel powders calcined at different temperatures corresponds to (a) precursor prepared by the γ-SGAP method and (b) precursor obtained by the SGAP method.

Table 1
Average grain size determined by the the Scherrer equation using the FWHM from XRD pattern.

Temperature (°C)	Size	
	SGAP (nm)	γ-SGAP (nm)
600	25.3	16.1
900	62.9	80.8

samples produced by the γ-SGAP and SGAP methods, respectively. Broad XRD peaks at temperatures lower than 900 °C indicate the nanocrystalline nature of the synthesized powders. It is worth noting that the crystallite sizes obtained by the γ-SGAP method are smaller than those obtained by the SGAP method. It can be observed that the widths of the XRD reflections at 900 °C are narrower than the widths found at lower temperatures. This occurred because further heating produced a increase in particle size. The diffraction peaks of the powders calcined at 900 °C (top side of Fig. 4a and b) are indexed to the rhombohedral structures with the R3c space group, referring to the standard diffraction data JCPDS 01-084-0848.

4.3. Analysis SEM of xerogel and LaCoO3 powder obtained by the γ-SGAP and SGAP methods

Fig. 4 shows SEM micrographs of the LCO xerogel obtained by γ-SGAP and SGAP methods. Differences in the morphology of the precursors can be observed in these images. The xerogel obtained by the γ-SGAP (Fig. 4a) method shows a compact and regular surface in which a porous structure is not observed. The xerogel obtained by SGAP (Fig. 4b) presents a structure with small pores. It also exhibits an unorganized clustered structure. We think that the differences in the structural features of both xerogels depend strongly of the way as crosslinking is achieved. Rüchel et al. (1978) report differences in the morphology of polyacrylamide gels obtained by varying the concentration between monomers and crosslinking agent. In the case of polymerization of acrylamide by irradiation method, it is believed that the irradiation dosage during hydrogel synthesis is the main controlling variable to obtain xerogels with different surfaces and morphology (Ulanski and Rosiak, 1999). The compact surface in xerogel obtained by the γ-SGAP method is achieved because γ-ray is a powerful ionizing radiation that promotes the crosslinking because the polymerization reaction begins in multiple sites of acrylamide chains (Alam et al., 2003).

Fig. 5 shows SEM micrographs of LCO powder synthesized by the γ-SGAP and SGAP methods and calcined at 700 °C (Fig. 5a and b). The images show some differences in grain morphology of LCO samples obtained by both methods. Additionally, it has to be pointed out that powders obtained by both methods show an amorphous phase that covers the grain surface. According to the FTIR spectra of precursors at 700 °C, this amorphous phase could be organic impurities that remained in final product. To remove all organic matter and other impurities it was necessary to heat the samples to 900 °C during 4 h.

4.4. Analysis of AFM images of xerogel

Fig. 6 shows the AFM images of xerogels obtained by γ-SGAP and SGAP methods. Clear differences in the morphology and microstructure of the xerogels surface can be seen in the 2D AFM images (Fig. 6a and b). The xerogel obtained by γ-SGAP shows a surface formed by polyacrylamide aggregates with rod-shape morphology, whereas the xerogel synthesized from the SGAP method shows an irregular surface formed by small particles. Fig. 6c and d shows the 3D AFM images of xerogels produced by γ-SGAP and SGAP methods, respectively. The topography of 3D images reveals differences induced by the gelation procedure of polyacrylamide. The ways in which crosslinking was done in the hydrogel are the most important factors that influence the gel microstructure.

4.5. TEM analysis of $LaCoO_3$ powder obtained by γ-SGAP and SGAP methods

Fig. 7 shows the TEM micrographs of LCO perovskite powders synthesized by the γ-SGAP and SGAP methods (Fig. 7a and b) and calcined in air at 700 °C for 3 h. The powders were characterized by sphere-type particles with a non-homogenous size distribution for both samples. According to TEM micrographs, the primary particle sizes of samples produced by the γ-SGAP method are

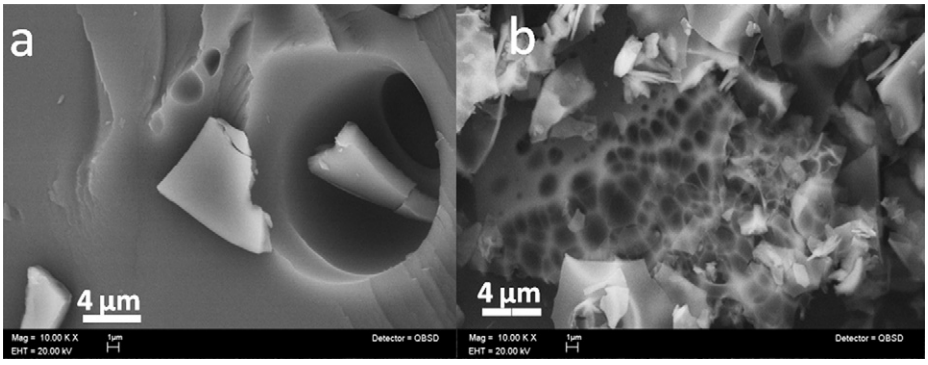

Fig. 4. SEM micrograph of the xerogel powder prepared by (a) the γ-SGAP and (b) the SGAP methods.

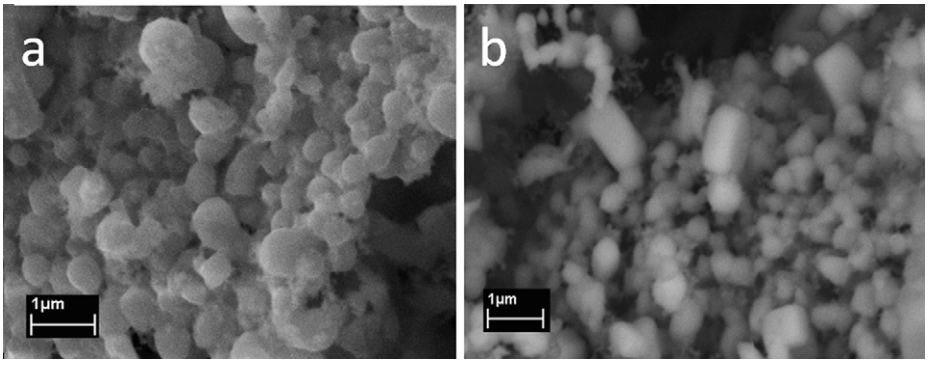

Fig. 5. SEM micrograph of the $LaCoO_3$ powders calcined at 700 °C, prepared by (a) the γ-SGAP and (b) the SGAP methods.

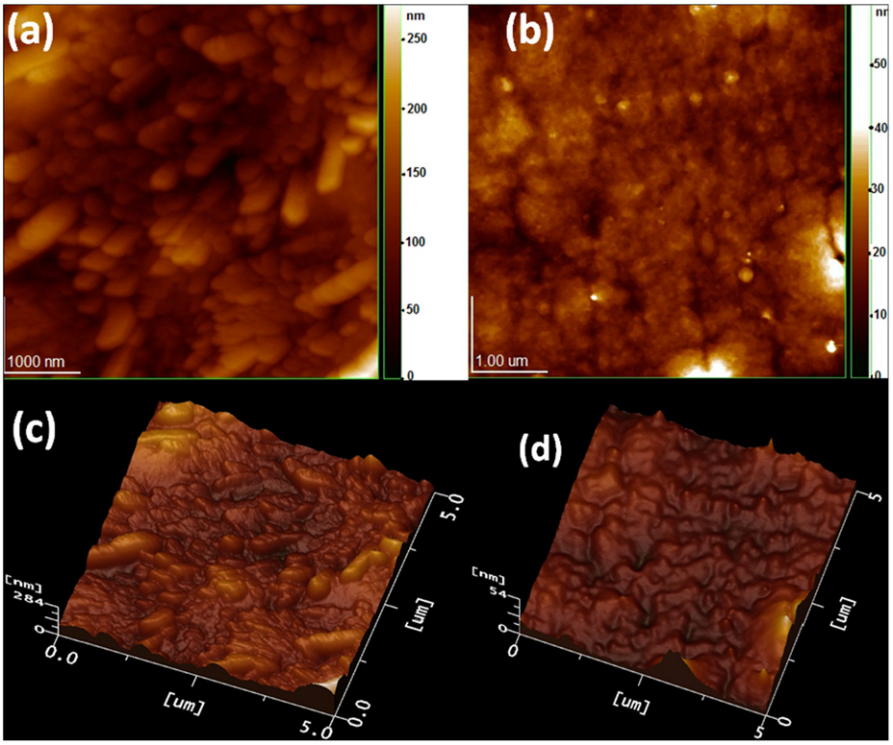

Fig. 6. AFM images of the xerogels. (a), (b) correspond to 2D AFM images of xerogel obtained by the γ-SGAP and SGAP methods, respectively. (c), (d) show the 3D AFM images to xerogels obtained by the γ-SGAP and SGAP methods.

about 20 nm. The average particle size measured to particles obtained by the method SGAP is 42 nm. In the TEM images, it is also possible to observe some differences in morphology and aggregation of particles. The particles synthesized by the γ-SGAP (Fig. 7a), have the smallest size and seem to be closely attached forming aggregates, those particles obtained by SGAP method

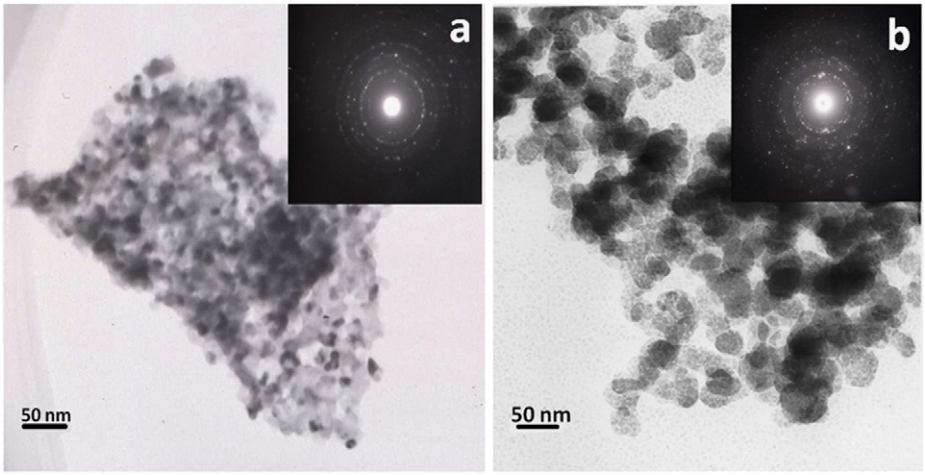

Fig. 7. TEM micrograph of the $LaCoO_3$ fine powders prepared by (a) the γ-SGAP and (b) the SGAP methods at the calcination temperature of 700 °C. In inset are shown the TEM diffraction pattern of each sample.

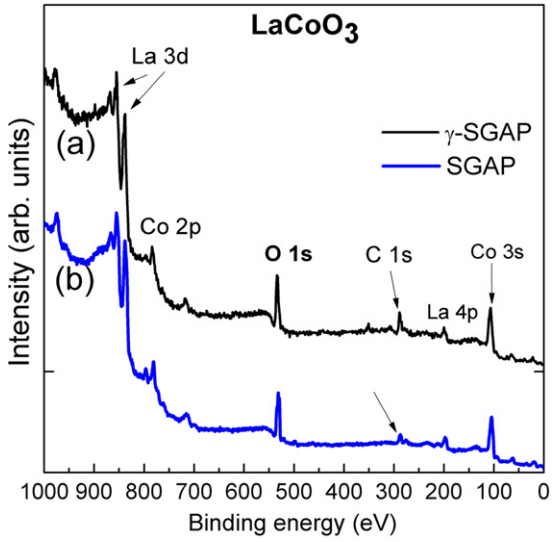

Fig. 8. Survey XP spectra of $LaCoO_3$ prepared by (a) the γ-SGAP and (b) the SGAP methods.

(Fig. 7b) have the largest size and appear to be dispersed. The insets in Fig. 7 show the TEM diffraction pattern of samples produced by both methods (γ-SGAP and SGAP). There are differences in both patters that can be associated to the size of the particle in each sample and to the particle size distribution. The TEM pattern also exhibits non-uniform bright rings that suggest that the nanocrystals have random orientations in the samples.

4.6. XPS analysis

The surface and chemical elemental compositions of the $LaCoO_3$ powders synthesized by the γ-SGAP and SGAP methods were studied by X-ray photoelectron spectroscopy (XPS). Fig. 8 shows the XPS survey spectra (binding energy of 0–1000 eV) where characteristic lines for La, Co and O are present. These spectra do not reveal the presence of extraneous species, except carbon. The presence of carbonate phases, which is the main drawback in the sol–gel techniques (Calleja et al., 2002) is observed in the survey XP spectra. The sample prepared by the γ-SGAP method shows a C1s signal more intense than the observed in the sample prepared by the SGAP method. This is due to the presence of carbon on the surfaces probably due to CO_2 adsorbed and contamination by handling the samples.

Fig. 9a and b shows the oxygen 1s (O-1s) and Cobalt 2p (Co-2p) XP spectra, respectively, of $LaCoO_3$ prepared by both methods. These spectra are in agreement to those reported in previous studies (Imamura et al., 2000). The O-1s XP spectra (Fig. 8a) show doublet features with the peak energies at 529.1 and 531.2 eV that according to Imamura et al. (2000) must be assigned to lattice oxygen and adsorbed oxygen species, respectively. It was reported, that this O1s higher binding energy feature corresponds to adsorbed oxygen-containing species. It can also be associated to the OH^- surface formed by water adsorption (Zhang-Steenwinkel et al., 2002). It is known that compounds with rare earth oxides become hygroscopic when exposed to ambient conditions (Li et al., 2004). The ratio between adsorbed oxygen and lattice oxygen O_S/O_L is slightly higher in particles obtained by the γ-SGAP method; this could be associated to a major surface area due to the small size of the particle.

In Fig. 9b the Co2p XPS spectra of LCO prepared by γ-SGAP and SGAP methods are presented. The spectra have $2p_{3/2}$ and $2p_{1/2}$ spin–orbit doublet peaks located at 780 and 796 eV, respectively. The absence of intense satellites in the Co2p XP spectra of the two samples indicated that Co(II) is not present. However, it is important to note the shape of the peaks in Co2p XP spectra of the compound synthesized by the γ-SGAP method show a broadening towards higher binding energies.

5. Conclusions

Powders of $LaCoO_3$ samples have been successfully synthesized using two different reactions: the conventional of sol–gel reaction of acrylamide polymerization activated by thermo-chemical initiator and a novel sol–gel methodology of polymerization of acrylamide initiated by gamma radiation. The dry gels (xerogeles) obtained by the two methodologies present different features that are induced by the way the reactions were initiated and the kind of cross-linking in the polymeric network. The analysis of SEM micrographs reveals some differences in structure of xerogeles synthesized by both methods. The xerogel obtained by the SGAP method has a foamy nature and porous structure, while that the xerogel obtained by the γ-SGAP method consist in a very compact resin in which porous structure is not observed. Also differences in calcinations temperatures were observed by thermogravimetrical analysis, where organic matter in xerogel produced by the γ-SGAP method

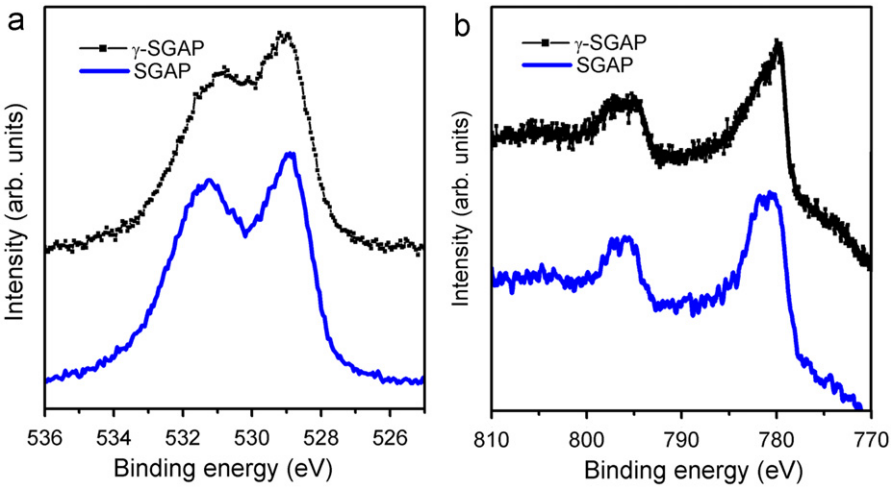

Fig. 9. XP spectra of (a) oxygen 1s and (b) cobalt 2p of $LaCoO_3$ powders prepared by the γ-SGAP and the SGAP methods.

burned at a higher temperature. The compact surface in xerogel obtained by the γ-SGAP method could be achieved because γ-ray is a powerful ionizing radiation that lets the polymerization reaction begin in multiple sites of acrylamide chains. Also, cations within the polymeric network could enhance the crosslinking behavior.

We also observed significant morphological differences between LCO powders. Specifically, the agglomeration of particles varies according to the method used in the synthesis. The TEM micrographs show that LCO particles obtained by the γ-SGAP method have a size of 20 nm and form agglomerates; in contrast, LCO particles synthesized by SGAP are more dispersed with particles size of 42 nm.

The novel γ-SGAP method utilized for the preparation of perovskite-type $LaCoO_3$ nanocrystals was found to be convenient and versatile. It also provided powders with nanometer sizes. The γ-SGAP shows good results and there are many variables that could be changed to control size and morphology of the powders. For example, one can vary the concentration of acrylamide and the dose of gamma radiation to change gel texture that can influence the properties of final powder. This method can be potentially adopted for the preparation of other complex oxides.

Acknowledgments

The authors would like to acknowledge financial support from CONACyT project 80380. We would like to thank to Carlos Flores for his technical support in TEM and AFM analysis of powders.

References

Alam, M.M., Mina, M.F., Akhtar, F., 2003. Effect of gamma rays in the preparation of polymer and hydrogel from acrylamide monomer. Chin. J. Polym. Sci. 21, 437–442.

Brinker, C.J., Scherer, G.W., 1990. Sol–Gel Science: The Physics and Chemistry of Sol–Gel Processing. Academic Press, San Diego.

Calleja, A., Casas, X., Serradilla, I.G., Segarra, M., Sin, A., Odier, P., Espiell, F., 2002. Up-scaling of superconductor powders by the acrylamide polymerization method. Physica C 372, 1115–1118.

Calleja, A., Capdevila, X.G., Segarra, M., Frontera, C., Espiell, F., 2011. Cation order enhancement in Sr_2FeMoO_6 by water-saturated hydrogen reduction. J. Eur. Ceram. Soc. 31, 121–127.

Chainani, A., Mathew, M., Sarma, D.D., 1992. Electron-spectroscopy study of the semiconductor–metal transition in $La_{1-x}Sr_xCoO_3$. Phys. Rev. B 46, 9976–9983.

Cheng, C.S., Zhang, L., Zhang, Y.J., Jiang, S.P., 2008. Synthesis of $LaCoO_3$ nanopowders by aqueous gel-casting for intermediate temperature solid oxide fuel cells. Solid State Ionics 179, 282–289.

Colonna, S., De Rossi, S., Faticanti, M., Pettiti, I., Porta, P., 2002. Zirconia supported La, Co oxides and $LaCoO_3$ perovskite: structural characterization and catalytic CO oxidation. J. Mol. Catal. A: Chem. 180, 161–168.

Haas, O., Struis, R.P.W.J., McBreen, J.M., 2004. Synchrotron X-ray absorption of $LaCoO_3$ perovskite. J. Solid State Chem. 177, 1000–1010.

Herrera, G., Chavira, E., Jimenez-Mier, J., Baños, L., Guzmán, J., Flores, C., 2008. Synthesis and structural characterization of YVO_3 prepared by sol–gel acrylamide polymerization and solid state reaction methods. J. Sol–Gel Sci. Technol. 46, 1–10.

Herrera, G., Chavira, E., Jimenez-Mier, J., Ordoñez, A., Fregoso-Israel, E., Baños, L., Bucio, E., Guzmán, J., Noelo, O., Flores, C., 2009. Structural and morphology comparison between m-$LaVO_4$ and $LaVO_3$ compounds prepared by sol–gel acrylamide polymerization and solid state reaction. J. Alloys Compd. 479, 511–519.

Holzwarth, U., Gibson, N., 2011. The Scherrer equation versus the 'Debye–Scherrer equation'. Nat. Nanotechnol. 6, 534.

Imamura, M., Matsubayashi, N., Shimada, H., 2000. Catalytically active oxygen species in $La_{1-x}Sr_xCoO_{3-\delta}$ studied by XPS and XAFS spectroscopy. J. Phys. Chem. B 104, 7348–7353.

Kim, C.H., Qi, G., Dahlberg, K., Li, W., 2010. Strontium-doped perovskites rival platinum catalysts for treating NO_x in simulated diesel exhaust. Science 327, 1624–1627.

Li, Y., Chen, N., Zhou, J., Song, S., Liu, L., Yin, Z., Cai, C., 2004. Effect of the oxygen concentration on the properties of Gd_2O_3 thin films. J. Cryst. Growth 265, 548–552.

Peña, M.A., Fierro, J.L.G., 2001. Chemical structures and performance of perovskite oxides. Chem. Rev. 101, 1981–2017.

Rüchel, R., Steere, R.L., Erbe, E.F., 1978. Transmission-electron microscopic observations of freeze-etched polyacrylamide gels. J. Chromatogr. 166, 563–575.

Scofield, J.H., 1976. Hartree–Slater subshell photoionization cross-sections at 1254 and 1487 eV. J. Electron Spectrosc. Relat. Phenom. 8, 129–137.

Sin, A., El Montaser, B., Odier, P., 2003. Nanopowders by organic polymerisation. J. Sol–Gel Sci. Technol. 26, 541–545.

Sin, A., Odier, P., 2000. Gelation by acrylamide, a quasi-universal medium for the synthesis of fine oxide powders for electroceramic applications. Adv. Mater. 12, 649–652.

Ulanski, P., Rosiak, J.M., 1999. The use of radiation technique in the synthesis of polymeric nanogels. Nucl. Instrum. Methods Phys. Res. Sect. B 151, 356–360.

Voorhoeve, R.J.H., Johnson Jr, D.W., Remeika, J.P., Gallagher, P.K., 1977. Perovskite oxides: materials science in catalysis. Science 195, 827–833.

Warren, B.E., 1990. X-ray Diffraction, second ed. Dover, New York.

Zhang-Steenwinkel, Y., Beckers, J., Bliek, A., 2002. Surface properties and catalytic performance in CO oxidation of cerium substituted lanthanum-manganese oxides. Appl. Catal. A 235, 79–92.